Electronic Supplementary Material (ESI) for Nanoscale Advances.

Electronic Supplementary Information on: Growing sp^2 materials on transition metals: Calculated atomic adsorption energies of hydrogen, boron, carbon, nitrogen, and oxygen atoms, C_2 and BN dimers, C_6 and $(BN)_3$ hexamers, graphene and h-BN with and without atomic vacancies

Ari Paavo Seitsonen[1] and Thomas Greber[2]

[1] *Département de Chimie, École Normale Supérieure, F-75005 Paris, France*

[2] *Physik-Institut, Universität Zürich, CH-8057 Zürich, Switzerland*[*]

[*] greber@physik.uzh.ch

CONTENTS

I. METHODS USED IN THE CALCULATIONS

The software package `Quantum ESPRESSO` [1, 2] was used in all the calculations. We apply a van der Waals density functional [3] as the appproximation of the exchange-correlation term in the Kohn-Sham equations.

We employed the grid of 18×18, 6×6 and 4×4 $\mathbf{k}$ points in the (1×1), (3×3) and (5×5) lateral super-cells, respectively. A cut-off energy of 60 Ry on the wave functions and of 480 Ry on the density were used in the plane wave basis, and more than 10 Å of a vacuum region separated the over-layers from the periodic image of the bottom of the slab. Slab geometries of the surfaces were used with five atomic layers of the support out of which three bottom-most ones were fixed during the optimisation of the geometry.

In Ref [4] the Authors calculated the solvation energy of atoms in bulk crystals. In avoid to having to perform the same, very similar calculations with the only difference being the slightly differing computational approach, and in particular the different approximation in the exchange-correlation, we calculated the same quantities in some cases without approach and fitted the difference with a linear model between the two approaches. Precisely we calculated the solvation energy of the B, C and N in bulk Ni, Cu and Rh both at the octahedral and tetrahedral sites, and fitted the six values on each solute atom independently. We obtain the following correspondences:

$$\text{B:}\quad E_{\text{sol}}^{\text{B;our}} = 0.9909\, E_{\text{sol}}^{\text{B;ref}} + 0.07766$$

$$\text{C:}\quad E_{\text{sol}}^{\text{C;our}} = 1.015\, E_{\text{sol}}^{\text{C;ref}} - 0.04379$$

$$\text{N:}\quad E_{\text{sol}}^{\text{N;our}} = 1.043\, E_{\text{sol}}^{\text{N;ref}} - 0.2305$$

where the values $E_{\rm sol}^{\rm ref}$, calculated with the approximation PBE, are taken from the Supporting Material of Ref [4]. The scatter in the data between their and our data is quite small and accordingly the fits are good.

II. ON THE CHOICE OF THE CHEMICAL POTENTIAL

Some further words about the choice of the choice of the value of the chemical potential: Throughtout the Main Text we have used the convertion of selecting the chemical potential of free atoms in the gas phase in the evaluation of the energetics. We mentioned another potential choice, the total energy of a N atom in the N_2 dimer. Here we discuss how the values that we have expressed would change if the other reference of the chemical potential was used.

In the case of graphene an obvious choice would be the total energy of a C atom in bulk C, such as bulk diamond, bulk graphite and a mono-layer of graphene. As the energy differences among those are small and the latter, graphene, is thematically closest to our investigations here, we show this as an example. The difference in the energy, $E_{\mathrm{C}}(\mathrm{gr}) - E_{\mathrm{C}}(\mathrm{atom})$, is the cohesive energy of graphene, $E_{\mathrm{coh}}(\mathrm{gr})$, equal to -7.754 eV in our computational setup. Thus the energetic values with the chemical potential of graphene $\mu_{\mathrm{C}}(\mathrm{gr})$ can be obtained by subtracting the value $E_{\mathrm{coh}}(\mathrm{gr})$ from our values in the Main Text; as an example the value of $E_{\mathrm{ads}}^{\mathrm{C_6}}(\mathrm{Ni})$ would be $(-7.072 + 7.754)$ eV $= 0.682$ eV when using $\mu_{\mathrm{C}}(\mathrm{gr})$. The case of h-BN is somewhat more complicated because the chemical potential of either B or N is in general not known, and in the experiments it would depend on the conditions during the growth of the sample. The thermodynamic formalism using values from DFT calculations have been derived and published many times, for example in the context of defects in compound semi-conductors, surfaces and so on; here we repeat the main points of the method and then give practical values.

In h-BN we do not know the individual values of the chemical potentials μ_{B}, μ_{N} of the B and the N and thus in principle we have two unknown parametres in our evaluation. Assuming ther formation of the h-BN the two are, however, related via $\mu_{\mathrm{B}} + \mu_{\mathrm{N}} = \mu_{h-\mathrm{BN}}$, which equals to $2E_{\mathrm{coh},h\text{-BN}} = 2 * -6.938$ eV in our calculations; thus we are left with one independent chemical potential. The factor two appears because we refer to our cohesive energy per atom. Its possible values are further limited from above and below assuming that no precipitation occurs; as the limiting cases we employ the bulk B and the nitrogen dimer N_2 here. The two chemical potentials are limited by the cohesive energy of the corresponding energy reference, here the α rhombohedral bulk crystal of B and the nitrogen dimer N_2, to

avoid precipitation into those forms:

$$\begin{aligned} \mu_{\mathrm{B}} &< E_{\mathrm{coh,B}} \ , \\ \mu_{\mathrm{N}} &< E_{\mathrm{coh,N}} \ . \end{aligned} \tag{1}$$

We manipulate the second Equation,

$$\begin{aligned} \mu_{\mathrm{N}} - 2E_{\mathrm{coh},h\text{-BN}} &< E_{\mathrm{coh,N}} - 2E_{\mathrm{coh},h\text{-BN}} \ , \\ -\mu_{\mathrm{B}} &< E_{\mathrm{coh,N}} - 2E_{\mathrm{coh},h\text{-BN}} \ , \\ \mu_{\mathrm{B}} &> 2E_{\mathrm{coh},h\text{-BN}} - E_{\mathrm{coh,N}} \ , \\ 2E_{\mathrm{coh},h\text{-BN}} - E_{\mathrm{coh,N}} &< \mu_{\mathrm{B}} \ . \end{aligned} \tag{2}$$

Thus we are left with the boundaries of μ_{B}, and the corresponding boundaries on μ_{N},

$$\begin{aligned} 2E_{\mathrm{coh},h\text{-BN}} - E_{\mathrm{coh,N}} < \mu_{\mathrm{B}} < E_{\mathrm{coh,B}} \ , \\ 2E_{\mathrm{coh},h\text{-BN}} - E_{\mathrm{coh,B}} < \mu_{\mathrm{N}} < E_{\mathrm{coh,N}} \ . \end{aligned} \tag{3}$$

With our values

$$\begin{aligned} -8.829 \text{ eV} < \mu_{\mathrm{B}} < -6.206 \text{ eV} \ . \\ -7.670 \text{ eV} < \mu_{\mathrm{N}} < -5.047 \text{ eV} \ . \end{aligned} \tag{4}$$

When the value of μ_{B} is close to the $E_{\mathrm{coh,B}}$ ($\mu_{\mathrm{B}} = -6.206$ eV, $\mu_{\mathrm{N}} = -7.670$ eV) one speaks of the *B-rich limit* and correspondingly of the *N-rich* limit when $\mu_{\mathrm{N}} = E_{\mathrm{coh,N}}$ ($\mu_{\mathrm{B}} = -8.829$ eV, $\mu_{\mathrm{N}} = -5.047$ eV). With these values we can express the energetics in the Main Text with respect to the B- and N-rich limits by subtracting the value of μ_{B} or μ_{N} eV, respectively, in Equations 1 and 3, and adding it in Equations 10 and 11. Therefore, as an example, the energy $E^{\mathrm{B}}_{\mathrm{ads}}$(Ni) in Table 1 would be $5.747 - 6.206$ eV $= -0.459$ eV at the B-rich limit and $(5.747 - 8.829)$ eV $= -3.085$ eV at the N-rich limit. The energies of the vacancies in the (1×1) layers will be listed below.

III. ADDITIONAL DATA FROM THE CALCULATIONS

In Table S1 we show further values computed with our approach:

- Calculated values of the lattice constant a – in hcp cells a and c –; the calculated lattice constant calculated with the approximation PBE a_{PBE}, the experimental lattice constant with the zero-point movement removed $a_{\mathrm{expt}} - \Delta a$ (the experimental lattice constant a_{expt}); the values of a_{PBE}, $a_{\mathrm{expt}} - \Delta a$, a_{expt} are from Ref [5];

- The mismatch of the calculated lattice constant with respect to the calculated value in graphene and in h-BN; the computed lattice constant in plane d; the incommensurability with respect to graphene and h-BN $d/a_{\mathrm{gr}} - 1$ and $d/a_{h-\mathrm{BN}} - 1$;

- The dissociation (or, negative of cohesive) energies $E_{\mathrm{diss}}^{\mathrm{gr}^*}$ and $E_{\mathrm{diss}}^{h\text{-}\mathrm{BN}^*}$, per atom calculated at the lattice constant of the supporting metal

When comparing the computed and the experimental lattice constants, unless an approach to account for the zero-point motion is applied we should rather compare to values $a_{\mathrm{expt}} - \Delta a$, where the term Δa removes an approximated zero-point motion, because the lattice constants from the computations do not contain the latter.

The energy of incommensurability, or the energy penalty due to the strain on the monolayer, can be evaluated as $E_{\mathrm{diss}}^{\mathrm{2D}^*} - E_{\mathrm{diss}}^{\mathrm{2D}}$, where the latter term is calculated at the optimal lattice constant and corresponds to the negative of the cohesive energy of the 2D layer.

TABLE S1. Calculated values of the lattice constant a – in hcp cells a and c –; the calculated lattice constant calculated with the approximation PBE a_{PBE}, the experimental lattice constant with the zero-point movement removed $a_{\mathrm{expt}} - \Delta a$ (the experimental lattice constant a_{expt}); the mismatch of the calculated lattice constant with respect to the calculated value in graphene and in h-BN; the computed lattice constant in plane d; the incommensurability with respect to graphene and h-BN $d/a_{\mathrm{gr}} - 1$ and $d/a_{h-\mathrm{BN}} - 1$; the dissociation (or, negative of cohesive) energies $E_{\mathrm{diss}}^{\mathrm{gr}^*}$ and $E_{\mathrm{diss}}^{h\text{-}\mathrm{BN}^*}$, per atom calculated at the lattice constant of the supporting metal. The values of a_{PBE}, $a_{\mathrm{expt}} - \Delta a$, a_{expt} are from Ref [5]. The lattice constants are in Å, γ in % and the energies in eV

Substrate	a, c	a_{PBE}	$a_{\mathrm{expt}} - \Delta a$	(a_{expt})	d	γ_{gr}	$\gamma_{h-\mathrm{BN}}$	$E_{\mathrm{diss}}^{\mathrm{gr}^*}$	$E_{\mathrm{diss}}^{h\text{-}\mathrm{BN}^*}$
gr	2.4644							−7.754	
h-BN	2.5116								−6.938
Co (hcp)	2.4756, 3.9996				2.476	0.5	−1.4	−7.753	−6.925
Co (fcc)	3.4946				2.471	0.3	−1.6	−7.754	−6.921
Ni	3.4921	3.517	3.509	(3.516)	2.469	0.2	−1.7	−7.754	−6.920
Cu	3.5913	3.630	3.595	(3.603)	2.539	3.0	1.1	−7.696	−6.931
Ru	2.7087, 4.2755				2.709	9.9	7.8	−7.234	−6.634
Rh	3.8088	3.827	3.793	(3.798)	2.693	9.3	7.2	−7.291	−6.676
Pd	3.9109	3.932	3.876	(3.881)	2.765	12.2	10.1	−7.007	−6.461
Ag	4.0964	4.150	4.063	(4.069)	2.897	17.5	15.3	−6.401	−5.968
Re	2.7613, 4.4557				2.761	12.0	9.9	−7.025	−6.474
Os	2.7431, 4.3304				2.743	11.3	9.2	−7.100	−6.532
Ir	3.9477	3.872	3.832	(3.835)	2.791	13.3	11.1	−7.158	−6.577
Pt	3.8587	3.971	3.913	(3.916)	2.729	10.7	8.6	−6.895	−6.372
Au	4.1173	4.147	4.061	(4.065)	2.911	18.1	15.9	−6.328	−5.907

Next we tabulate the solvation, adsorption, bond and vacancy defect energies where we include all the calculated sites, whereas in the Main Text we only gave data at the lowest energy sites, which are emphasised here.

- Table S2: The solvation energies of B, C and N in bulk crystals and the adsorption energy of atomic H, B, C, N and O (eV per atom) on the studied surfaces. The solution energies of B, C and N are inferred from Ref [4]

- Table S3: The adsorption and dissociation energies and lowest energy adsorption sites of the dimers C_2 and BN

- Tables S4 and S5: The adsorption $E_{\rm ads}^{\rm hex}$ and single bond-dissociation energies $E_{\rm 6bo}^{\rm hex}$ and lowest energy adsorption sites of the C_6 and $(BN)_3$ ring-hexamers

- Tables S6 and S7: The adsorption energies of strained graphene and h-BN

- Table S8: Vacancy defect energies in graphene and h-BN on the studied surfaces and without the substrate with the value of the chemical potential $\mu_{\rm C}$(gr) and at the limits of the $\mu_{\rm B,N}$(B-rich) and $\mu_{\rm B,N}$(N-rich)

Comparing the registry of the adsorption sites of the monomer, dimer, ring-hexamer and the full mono-layer we see that whereas the monomer and dimer still prefer to adsorb on the three-fold hollow sites, on most of the surfaces of the $4d$ and $5d$ metals the hexamer takes a registry where the nitrogen is on top of a substrate atoms, and by the time the first layer is completed only on the surface of gold the boron atoms prefers to stay on top of the surface atom in the case of h-BN, whereas on all the other surfaces the nitrogen assumes the on top position.

We find that the vacancy formation energies in the free standing graphene in Table S8 can now be easily compared to the values in the literature, for example $E_{\rm vac}^{\rm C} = (7.3 - 7.5)$ eV are listed in Ref [6], which compare favourable with our value of 7.85 eV, in particular considering the small unit cell employed in our calculations.

We combined the favoured energies into the Figure S2, in which the energies of the solvated species, C_s and $(B{+}N)_s$, the adsorbed monomers, C_1 and B+N, dimers, C_2 and BN, hexamers C_6 and $(BN)_3$, and the strained mono-layer, gr and h-BN, are depicted in single graphs. The energies are referred to free atoms in the gas phase, and the evolution

of the growth would proceed from the monomers toward the mono-layer. If the initial deposition is performed as adsorbed atoms, the epiphilicity or epiphobicity would determine whether the atoms would rather be solvated into the bulk, left from the adsorbed monomer in the graphs, or proceed to growing seeds, toward to the right. From the graphs it is also visible which species would rather remain as monomers rather than associate to the larger clusters on the surface. We note that a different choice of the chemical potential $\mu_{\mathrm{B,C,N}}$ corresponds to a vertical shift of the zero, or the reference, of all the energies yielding the zero at the chosen reference; here the reference is at the energy of the free atoms.

TABLE S2. Adsorption energy of atomic H, B, C, N and O (eV per atom) on the studied surfaces

		E_{sol}		E_{ads}				E_{diff}
Adsorbate	Substrate	oct	tet	fcc	hcp	top	bridge	
H	Co (hcp)			**−2.990**	−2.955	−2.378	−2.832	0.157
	Co (fcc)			**−2.978**	−2.955	−2.375	−2.831	0.148
	Ni			**−2.978**	−2.963	−2.438	−2.843	0.135
	Cu			**−2.692**	−2.689	−2.119	−2.566	0.127
	Ru			**−3.042**	−2.964	−2.617	−2.899	0.143
	Rh			**−2.980**	−2.945	−2.666	−2.872	0.108
	Pd			**−2.985**	−2.937	−2.511	−2.851	0.134
	Ag			**−2.282**	−2.277	−1.802	−2.174	0.108
	Re			**−3.095**	−3.068	−2.378	−2.908	0.187
	Os			**−2.924**	−2.833	−2.818	−2.832	0.091
	Ir			−2.833	−2.800	**−2.943**	−2.801	0.109
	Pt			−2.874	−2.819	**−2.935**	−2.845	0.061
	Au			**−2.323**	−2.293	−2.148	−2.269	0.054
B	Co (hcp)	**−5.514**	−3.800	−5.577	**−5.690**	−4.067	−5.526	0.164
	Co (fcc)			−5.565	**−5.701**	−4.068	−5.533	0.169
	Ni	**−6.019**	−4.226	−5.678	**−5.747**	−4.008	−5.522	0.225
	Cu	**−4.632**	−3.265	**−4.287**	−4.261	−2.908	−4.268	0.026
	Ru	**−5.098**	−3.393	−5.808	**−6.302**	−4.118	−5.800	0.502
	Rh	**−6.386**	−4.295	−6.207	**−6.439**	−4.402	−5.985	0.454
	Pd	**−7.268**	−5.930	−6.303	**−6.364**	−4.181	−5.972	0.392
	Ag	**−3.720**	−2.739	**−3.447**	−3.421	−2.234	−3.328	0.119
	Re	**−6.109**	−3.661	**−5.826**	−5.784	−3.586	−5.626	0.200
	Os	**−4.295**	−2.224	−5.848	**−6.495**	−3.943	−5.880	0.648
	Ir	**−5.365**	−3.166	−6.280	**−6.562**	−4.339	−6.008	0.554
	Pt	**−6.554**	−5.593	−6.656	**−6.676**	−4.432	−6.246	0.431
	Au	**−4.424**	−3.869	**−4.754**	−4.692	−2.923	−4.479	0.275
C	Co (hcp)	**−6.955**	−5.291	−6.884	**−7.075**	−4.962	−6.725	0.349
	Co (fcc)			−6.866	**−7.072**	−4.939	−6.717	0.355
	Ni	**−7.128**	−5.413	−6.788	**−6.826**	−4.437	−6.448	0.377
	Cu	**−5.179**	−3.789	**−5.010**	−4.950	−3.072	−4.913	0.097
	Ru	**−5.971**	−4.783	−7.021	**−7.715**	−5.403	−6.941	0.774
	Rh	**−6.823**	−5.443	−7.211	**−7.406**	−5.378	−6.763	0.643
	Pd	**−7.290**	−6.509	−6.963	**−6.975**	−4.339	−6.542	0.432
	Ag	**−3.575**	−2.784	**−3.638**	−3.557	−2.065	−3.409	0.229
	Re	**−7.554**	−5.494	−7.351	**−7.575**	−4.711	−7.123	0.452
	Os	**−4.854**	−3.728	−6.972	**−7.868**	−5.327	−6.957	0.911
	Ir	**−5.260**	−4.489	−7.078	**−7.331**	−5.611	−6.617	0.714
	Pt	−5.991	**−6.174**	**−7.196**	−7.074	−4.927	−6.861	0.335
	Au	−3.393	**−3.515**	**−4.665**	−4.526	−2.584	−4.403	0.262
N	Co (hcp)	**−4.704**	−3.525	−5.677	**−5.836**	−3.538	−5.317	0.519
	Co (fcc)			−5.660	**−5.812**	−3.513	−5.298	0.514
	Ni	**−4.527**	−3.411	**−5.410**	−5.355	−2.805	−4.908	0.501
	Cu	**−3.223**	−2.232	**−3.917**	−3.825	−1.786	−3.640	0.277
	Ru	**−3.191**	−2.962	−5.635	**−6.395**	−4.391	−5.501	0.894
	Rh	**−3.536**	−3.223	−5.499	**−5.629**	−3.581	−4.960	0.669
	Pd	**−3.817**	−3.744	**−4.895**	−4.853	−2.198	−4.464	0.431
	Ag	**−1.898**	−1.283	**−2.390**	−2.275	−0.670	−2.109	0.280
	Re	**−5.017**	−3.598	−6.284	**−6.788**	−4.602	−6.045	0.743
	Os	−1.544	**−1.961**	−5.528	**−6.455**	−4.637	−5.409	1.046
	Ir	−1.158	**−2.274**	−5.252	**−5.391**	−3.994	−4.708	0.683
	Pt	−1.731	**−3.233**	**−4.947**	−4.759	−2.631	−4.623	0.324
	Au	−0.834	**−1.314**	**−2.743**	−2.517	−0.726	−2.465	0.279
O	Co (hcp)			−5.814	**−5.837**	−4.283	−5.458	0.379
	Co (fcc)			−5.815	**−5.848**	−4.248	−5.451	0.397
	Ni			**−5.487**	−5.360	−3.590	−4.985	0.502
	Cu			**−4.870**	−4.779	−3.121	−4.536	0.334
	Ru			−5.741	**−6.150**	−4.683	−5.464	0.687
	Rh			**−5.255**	−5.190	−3.764	−4.758	0.497
	Pd			**−4.512**	−4.310	−2.828	−4.079	0.433
	Ag			**−3.716**	−3.616	−2.213	−3.430	0.286
	Re			−6.285	**−6.865**	−5.565	−6.000	0.865
	Os			−5.532	**−6.015**	−4.882	−5.244	0.771
	Ir			**−4.934**	−4.815	−3.935	−4.482	0.452
	Pt			**−4.392**	−3.998	−3.018	−4.018	0.393
	Au			**−3.312**	−3.078	−1.936	−3.049	0.263

TABLE S3. C_2 and BN dimer adsorption and dissociation energies and lowest energy adsorption sites on the studied surfaces. The dissociation energies of C_2 and BN in the gas phase are 6.000 and 4.620 eV. Energies in (eV/dimer)

	$C_{hcp}C_{fcc}$		$B_{hcp}N_{fcc}$		$B_{fcc}N_{hcp}$	
Substrate	E_{ads}^{CC}	E_{diss}^{CC}	E_{ads}^{BN}	E_{diss}^{BN}	E_{ads}^{BN}	E_{diss}^{BN}
gas phase	–	6.000	–	4.620	–	4.620
Co (hcp)	−8.335	0.185	**−7.387**	0.481	−7.379	0.473
Co (fcc)	−8.349	0.205	**−7.399**	0.506	−7.390	0.497
Ni	−8.034	0.382	**−7.123**	0.586	−7.059	0.522
Cu	−6.978	2.958	**−6.190**	2.606	−6.167	2.583
Ru	−8.656	−0.774	**−7.681**	−0.396	−7.643	−0.434
Rh	−8.115	−0.697	**−7.212**	−0.236	−7.071	−0.377
Pd	−7.241	−0.709	**−6.488**	−0.151	−6.346	−0.293
Ag	−5.830	4.554	**−5.199**	3.982	−5.191	3.974
Re	−9.250	0.100	−7.999	0.005	**−8.273**	0.279
Os	−8.629	−1.107	**−7.630**	−0.700	−7.581	−0.749
Ir	−7.855	−0.807	**−7.012**	−0.321	−6.809	−0.524
Pt	−7.303	−1.089	**−6.513**	−0.490	−6.513	−0.490
Au	−5.675	2.345	**−5.058**	2.181	−5.035	2.158

TABLE S4. The adsorption $E_{\mathrm{ads}}^{\mathrm{hex}}$ and single bond-dissociation energies $E_{\mathrm{6bo}}^{\mathrm{hex}}$ and lowest energy adsorption sites of the C_6 hexamer on the studied surfaces. The atomisation energy of the molecules is 34.304 eV. The energies are in (eV/hexamer) and (eV/bond)

	hcp,top		fcc,hcp		top,fcc	
Surface	$E_{\mathrm{ads}}^{\mathrm{hex}}$	$E_{\mathrm{6bo}}^{\mathrm{hex}}$	$E_{\mathrm{ads}}^{\mathrm{hex}}$	$E_{\mathrm{6bo}}^{\mathrm{hex}}$	$E_{\mathrm{ads}}^{\mathrm{hex}}$	$E_{\mathrm{6bo}}^{\mathrm{hex}}$
	–	5.717	–	5.717	–	5.717
Co (hcp)	−6.048	−0.350	**−7.915**	−0.039	−5.947	−0.367
Co (fcc)	−5.941	−0.365	**−7.924**	−0.034	−5.859	−0.378
Ni	−5.728	−0.154	**−7.072**	0.070	−5.692	−0.160
Cu	−3.737	1.330	**−4.146**	1.398	−3.694	1.323
Ru	−6.468	−0.920	**−7.743**	−0.707	−6.708	−0.880
Rh	−6.010	−0.687	**−6.053**	−0.680	−6.079	−0.676
Pd	**−5.411**	−0.356	−5.175	−0.395	−5.347	−0.367
Ag	**−2.285**	2.460	−2.009	2.414	−2.241	2.453
Re	−6.298	−0.808	**−8.823**	−0.387	−5.985	−0.860
Os	−6.254	−1.108	−6.488	−1.069	**−6.540**	−1.061
Ir	−5.657	−0.671	−3.940	−0.957	**−5.755**	−0.655
Pt	**−5.657**	−0.536	−3.461	−0.902	−5.616	−0.543
Au	**−2.760**	1.512	−0.639	1.159	−2.727	1.507

TABLE S5. The adsorption $E^{\text{hex}}_{\text{ads}}$ and single bond-dissociation energies $E^{\text{hex}}_{\text{6bo}}$ and lowest energy adsorption sites of the $(BN)_3$ hexamer on the studied surfaces. The atomisation energy of the molecules is 32.204 eV. The energies are in (eV/hexamer) and (eV/bond)

	fcc,top		hcp,top		top,hcp		fcc,hcp		top,fcc		hcp,fcc	
Surface	$E^{\text{hex}}_{\text{ads}}$	$E^{\text{hex}}_{\text{6bo}}$	$E^{\text{hex}}_{\text{ads}}$	$E^{\text{hex}}_{\text{6bo}}$	$E^{\text{hex}}_{\text{ads}}$	$E^{\text{hex}}_{\text{6bo}}$	$E^{\text{hex}}_{\text{ads}}$	$E^{\text{hex}}_{\text{6bo}}$	$E^{\text{hex}}_{\text{ads}}$	$E^{\text{hex}}_{\text{6bo}}$	$E^{\text{hex}}_{\text{ads}}$	$E^{\text{hex}}_{\text{6bo}}$
	–	5.367	–	5.367	–	5.367	–	5.367	–	5.367	–	5.367
Co (hcp)	−3.763	0.232	−3.824	0.242	−2.461	0.015	−4.239	0.311	−2.347	−0.005	**−4.277**	0.317
Co (fcc)	−3.654	0.220	−3.698	0.227	−2.418	0.014	−4.147	0.302	−2.296	−0.007	**−4.224**	0.315
Ni	−3.722	0.409	−3.749	0.414	−2.636	0.228	−3.707	0.407	−2.607	0.223	**−3.812**	0.424
Cu	−1.757	1.558	−1.754	1.558	−1.349	1.490	**−1.875**	1.578	−1.308	1.483	−1.842	1.572
Ru	−4.673	−0.202	**−4.701**	−0.198	−2.132	−0.626	−3.557	−0.388	−2.453	−0.572	−4.399	−0.248
Rh	−4.212	0.035	**−4.289**	0.048	−2.335	−0.278	−2.892	−0.185	−2.508	−0.249	−3.340	−0.110
Pd	−3.537	0.327	**−3.575**	0.334	−2.695	0.187	−2.846	0.212	−2.756	0.197	−2.973	0.233
Ag	**−0.785**	2.580	−0.783	2.579	−0.777	2.578	−0.606	2.550	−0.767	2.577	−0.585	2.546
Re	−4.544	−0.182	−4.630	−0.168	−1.511	−0.688	**−4.664**	−0.162	−1.296	−0.724	−4.527	−0.185
Os	−5.006	−0.273	**−5.070**	−0.263	−1.584	−0.844	−2.439	−0.701	−1.959	−0.781	−3.444	−0.534
Ir	−4.404	0.125	**−4.517**	0.144	−1.729	−0.321	−1.459	−0.366	−1.916	−0.290	−1.906	−0.292
Pt	−3.907	0.207	**−3.979**	0.219	−2.282	−0.064	−1.539	−0.188	−2.568	−0.016	−1.646	−0.170
Au	−0.862	1.763	−0.897	1.768	**−0.943**	1.776	−0.458	1.695	−0.920	1.772	−0.459	1.695

TABLE S6. Adsorption energies of strained graphene on the studied surfaces. Energies in (eV/(1×1) unit cell)

	$C_{fcc,top}$		$C_{hcp,top}$		$C_{fcc,hcp}$	
Substrate	E^{gr}_{ads}	$E^{gr}_{sp^2}$	E^{gr}_{ads}	$E^{gr}_{sp^2}$	E^{gr}_{ads}	$E^{gr}_{sp^2}$
Co (hcp)	**−0.284**	0.547	−0.275	0.544	−0.115	0.491
Co (fcc)	−0.133	0.499	**−0.232**	0.532	−0.114	0.493
Ni	**−0.158**	0.672	−0.135	0.664	−0.119	0.659
Cu	**−0.127**	1.834	−0.126	1.833	−0.115	1.830
Ru	**−0.874**	−0.029	−0.739	−0.074	−0.130	−0.277
Rh	**−0.576**	0.116	−0.498	0.090	−0.135	−0.031
Pd	**−0.558**	0.208	−0.526	0.198	−0.172	0.080
Ag	**−0.235**	1.921	−0.221	1.917	−0.150	1.893
Re	−0.929	−0.057	**−0.953**	−0.049	−0.129	−0.323
Os	**−0.856**	−0.226	−0.656	−0.293	−0.123	−0.471
Ir	**−0.441**	0.032	−0.360	0.005	−0.128	−0.072
Pt	**−0.432**	−0.056	−0.394	−0.069	−0.149	−0.150
Au	**−0.169**	1.166	−0.164	1.164	−0.142	1.157

TABLE S7. Adsorption energies of strained *h*-BN on the studied surfaces. Energies in (eV/(1×1) unit cell)

	$B_{fcc}N_{top}$		$B_{hcp}N_{top}$		$B_{top}N_{hcp}$		$B_{fcc}N_{hcp}$		$B_{top}N_{fcc}$		$B_{hcp}N_{fcc}$	
Substrate	$E^{h\text{-BN}}_{ads}$	$E^{h\text{-BN}}_{sp^2}$	$E^{h\text{-BN}}_{ads}$	$E^{h\text{-BN}}_{sp^2}$	$E^{h\text{-BN}}_{ads}$	$E^{h\text{-BN}}_{sp^2}$	$E^{h\text{-BN}}_{ads}$	$E^{h\text{-BN}}_{sp^2}$	$E^{h\text{-BN}}_{ads}$	$E^{h\text{-BN}}_{sp^2}$	$E^{h\text{-BN}}_{ads}$	$E^{h\text{-BN}}_{sp^2}$
Co (hcp)	**−0.302**	0.814	−0.302	0.814	−0.117	0.814	−0.117	0.814	−0.117	0.876	−0.117	0.876
Co (fcc)	**−0.263**	0.816	−0.263	0.816	−0.116	0.816	−0.116	0.816	−0.116	0.865	−0.116	0.865
Ni	**−0.172**	0.935	−0.163	0.935	−0.121	0.935	−0.120	0.935	−0.121	0.949	−0.120	0.952
Cu	**−0.132**	1.925	−0.132	1.926	−0.115	1.925	−0.114	1.925	−0.116	1.931	−0.115	1.931
Ru	**−0.794**	0.237	−0.774	0.237	−0.134	0.236	−0.135	0.236	−0.136	0.449	−0.136	0.456
Rh	**−0.517**	0.477	−0.491	0.481	−0.156	0.477	−0.146	0.481	−0.158	0.592	−0.146	0.601
Pd	**−0.392**	0.617	−0.373	0.664	−0.326	0.618	−0.190	0.663	−0.328	0.679	−0.187	0.685
Ag	**−0.171**	2.080	−0.169	2.082	−0.143	2.079	−0.137	2.081	−0.145	2.090	−0.138	2.091
Re	−1.030	0.159	**−1.094**	0.157	−0.134	0.158	−0.137	0.157	−0.135	0.477	−0.141	0.455
Os	**−0.837**	0.083	−0.806	0.083	−0.131	0.082	−0.130	0.083	−0.133	0.308	−0.131	0.318
Ir	**−0.426**	0.447	−0.383	0.455	−0.144	0.447	−0.137	0.449	−0.146	0.529	−0.137	0.543
Pt	**−0.259**	0.429	−0.229	0.459	−0.251	0.429	−0.163	0.458	−0.255	0.451	−0.163	0.461
Au	−0.179	1.491	−0.178	1.500	−0.179	1.491	−0.154	1.499	**−0.182**	1.499	−0.154	1.499

TABLE S8. Vacancy defect energies, in eV, in graphene and h-BN on the studied surfaces, $E_{\rm vac}^{\rm C,B,N}$, and without the substrate, $E_{\rm vac}^{\rm C,B,N}$(free). Here the value of the chemical potential $\mu_{\rm C}$(gr) and the limits of the $\mu_{\rm B,N}$(B-rich) and $\mu_{\rm B,N}$(N-rich) are used

	$\mu_{\rm C}$(gr)		$\mu_{\rm B,N}$(B-rich)				$\mu_{\rm B,N}$(N-rich)			
Substrate	$E_{\rm vac}^{\rm C*}$	$E_{\rm vac}^{\rm C*}$(free)	$E_{\rm vac}^{\rm B*}$	$E_{\rm vac}^{\rm B*}$(free)	$E_{\rm vac}^{\rm N*}$	$E_{\rm vac}^{\rm N*}$(free)	$E_{\rm vac}^{\rm B*}$	$E_{\rm vac}^{\rm B*}$(free)	$E_{\rm vac}^{\rm N*}$	$E_{\rm vac}^{\rm N*}$(free)
free	7.853		9.926		5.401		7.301		8.026	
Co (hcp)	2.250	7.893	5.622	9.933	0.819	4.960	2.996	7.308	3.445	7.585
Co (fcc)	2.179	7.886	5.518	9.924	0.742	4.893	2.893	7.299	3.367	7.518
Ni	2.611	7.882	5.611	9.920	0.917	4.867	2.986	7.295	3.542	7.492
Cu	4.724	7.729	6.225	9.833	3.471	5.644	3.599	7.208	6.096	8.269
Ru	0.982	5.761	3.120	8.121	0.564	5.474	0.495	5.496	3.189	8.100
Rh	0.775	6.012	3.534	8.358	0.470	5.597	0.909	5.732	3.095	8.223
Pd	0.837	4.726	2.996	7.178	−0.466	4.913	0.371	4.553	2.159	7.538
Ag	−1.583	1.255	0.084	4.499	0.142	3.099	−2.541	1.874	2.767	5.724
Re	−0.579	4.807	3.032	7.250	0.474	4.959	0.407	4.625	3.099	7.584
Os	0.607	5.155	2.177	7.562	−0.016	5.153	−0.448	4.937	2.610	7.778
Ir	0.095	5.420	2.177	7.804	−0.274	5.297	−0.448	5.179	2.351	7.922
Pt	−0.382	4.185	1.539	6.711	−1.940	4.607	−1.086	4.086	0.686	7.232
Au	−1.814	0.679	1.676	4.120	−1.232	2.843	−0.949	1.495	1.393	5.469

In Figure S1 we visualise the optimised geometry of the vacancies ($\overline{\rm B}$,N)=(fcc,top) and (B,$\overline{\rm N}$)=(fcc,top) on the Cu(111) and ($\overline{\rm B}$,N)=(top,fcc) on the Au(111) surfaces.

We provide the relaxed geometries and the input and output files from the calculations at the address `https://www.iki.fi/~apsi/Science/Projects/2D-layer/2D@TM/index.html`.

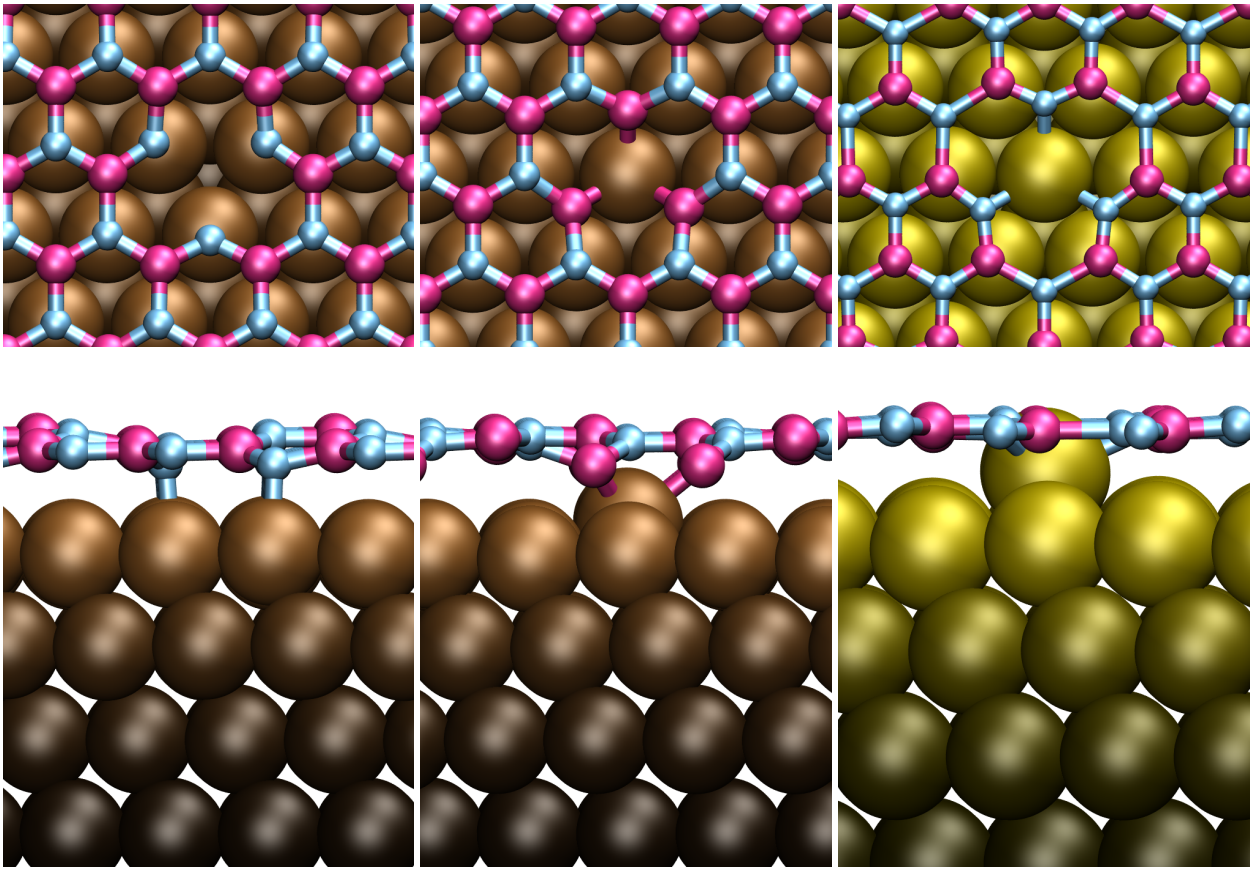

FIG. S1. Visualisation of the geometry of the vacancy ($\overline{\text{B}}$,N)=(fcc,top) – left panels – and (B,$\overline{\text{N}}$)=(fcc,top) – central panels – on the Cu(111) and ($\overline{\text{B}}$,N)=(top,fcc) on the Au(111) surface – right panels.

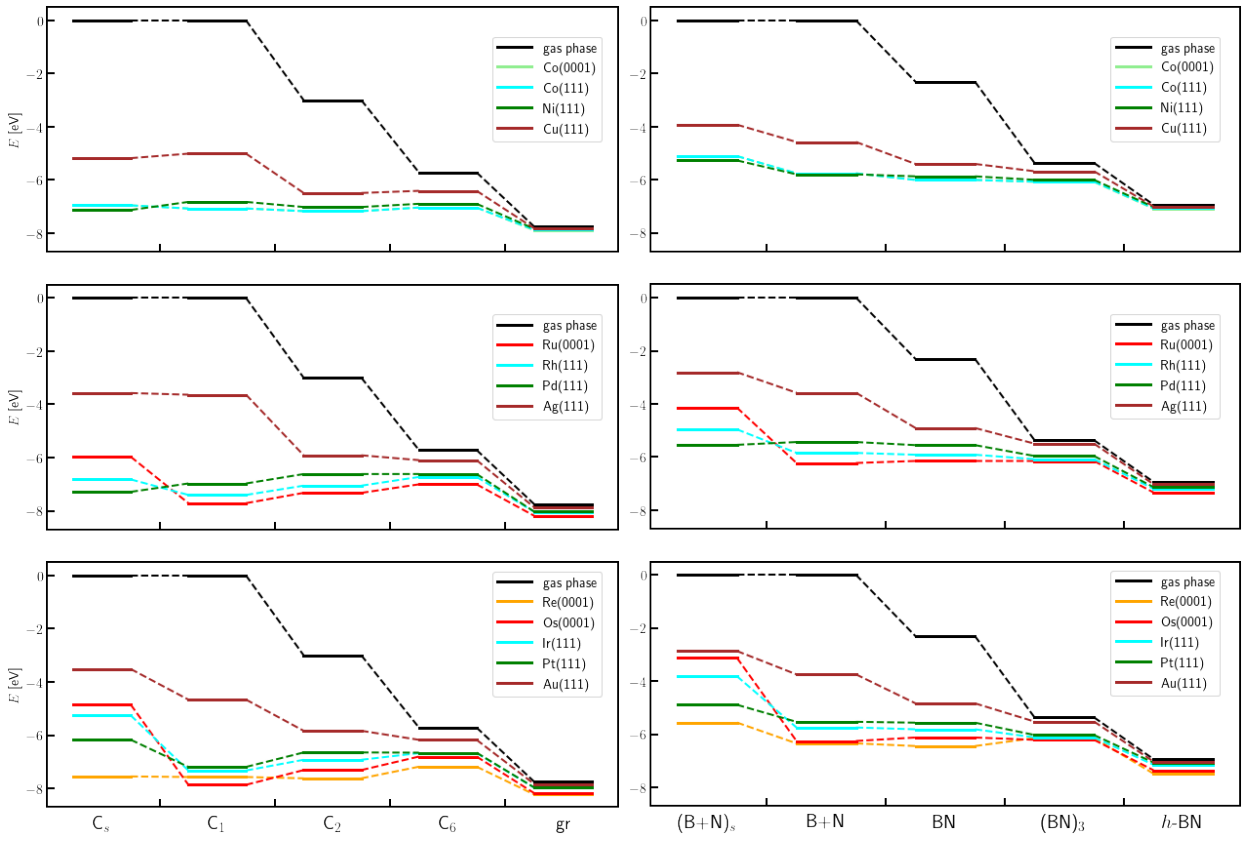

FIG. S2. Combined energy diagram of the carbon – left panels – and BN – right panels –, containing the solvation energy of the single atoms, the adsorption energies of the single atoms, the dimer and the hexamer and the adsorption energy of the strained 2D layers.

[1] https://www.Quantum-ESPRESSO.org/.

[2] P. Giannozzi, S. Baroni, N. Bonini, M. Calandra, R. Car, C. Cavazzoni, D. Ceresoli, G. L. Chiarotti, M. Cococcioni, I. Dabo, A. D. Corso, S. de Gironcoli, S. Fabris, G. Fratesi, R. Gebauer, U. Gerstmann, C. Gougoussis, A. Kokalj, M. Lazzeri, L. Martin-Samos, N. Marzari, F. Mauri, R. Mazzarello, S. Paolini, A. Pasquarello, L. Paulatto, C. Sbraccia, S. Scandolo, G. Sclauzero, A. P. Seitsonen, A. Smogunov, P. Umari and R. M. Wentzcovitch, *J. Phys.: Condens. Matter*, 2009, **21**, 395502.

[3] I. Hamada, *Phys. Rev. B*, 2014, **89**, 121103.

[4] X. Hu, T. Bjorkman, H. Lipsanen, L. Sun and A. Krasheninnikov, *Journal of Physical Chemistry Letters*, 2015, **6**, 3263–3268.

[5] P. Hao, Y. Fang, J. Sun, G. I. Csonka, P. H. T. Philipsen and J. P. Perdew, *Phys. Rev. B*, 2012, **85**, 014111.

[6] F. Banhart, J. Kotakoski and A. V. Krasheninnikov, *ACS Nano*, 2011, **5**, 26–41.